Pharmacological Research 185 (2022) 106489

Contents lists available at ScienceDirect

Pharmacological Research

journal homepage: www.elsevier.com/locate/yphrs

Nao Tan Qing ameliorates Alzheimer's disease-like pathology by regulating glycolipid metabolism and neuroinflammation: A network pharmacology analysis and biological validation

Qianqian Li [a], Caixia Jia [b], Hongxing Wu [a,b], Yajin Liao [c], Ke Yang [b], Shuoshuo Li [b], Jing Zhang [a], Jinlei Wang [d], Guo Li [d], Fangxia Guan [d], Elaine Leung [e], Zengqiang Yuan [a,*], Qian Hua [b,*], Rui-Yuan Pan [a,*]

[a] The Brain Science Center, Beijing Institute of Basic Medical Sciences, Beijing 100850, China
[b] School of Life Sciences, Beijing University of Chinese Medicine, Beijing 100029, China
[c] Department of neurology, The Second Affiliated Hospital, Hengyang Medical School, University of South China, Hengyang 42100, Hunan, China
[d] School of Life Sciences, Zhengzhou University, Zhengzhou 450001, Henan, China
[e] Cancer Center, Faculty of Health Science, University of Macau, Macau (SAR), China. MOE Frontiers Science Center for Precision Oncology, University of Macau, Macau (SAR), China

ARTICLE INFO

Keywords:
Alzheimer's disease
Systems pharmacology
Nao Tan Qing
Traditional Chinese medicine
Glycolipid metabolism
Neuroinflammation

ABSTRACT

Alzheimer's disease (AD) is a neurodegenerative disorder characterized by progressive cognitive decline and currently there are no available treatments. Alongside the conventional Aβ and tau hypotheses, neuroinflammation and metabolism disruption have also been regarded as crucial hallmarks of AD. In this study, a novel Chinese formula Nao Tan Qing (NTQ) was developed and shown to improve AD. *In vivo* experiments showed that NTQ significantly mitigated cognitive impairment, Aβ burden and neuroinflammation in a transgenic AD mouse model (5×FAD). Network pharmacology results revealed that the active components of NTQ could target inflammatory and metabolic pathways. In addition, hippocampal transcriptomics suggested that NTQ regulated signaling pathways related to inflammation and lipid metabolism. Consistently, serum metabolomics further indicated that NTQ could modulate glycolipid metabolism. In summary, a combination of systems pharmacology analysis and biological validation study demonstrates that NTQ could alleviate behavioral abnormality and pathological alterations of AD by targeting glycolipid metabolism and neuroinflammation, and is accordingly a potential therapeutic agent for AD.

1. Introduction

Alzheimer's disease (AD) is the most prevalent age-related neurodegenerative disease with insidious onset and slow progression. Considering that it affects approximately 46 million people worldwide and efficacious therapy remains unavailable at this moment, AD is becoming a global public health threat [1]. The initial stage of AD is marked by compromised ability to encode and store new memories, followed by a gradual deterioration of behavioral and cognitive functioning in later stages. A plethora of evidence supports that β amyloid (Aβ) and neurofibrillary tangles are two major culprits behind synaptic dysfunction, neuronal loss, and cognitive declines in AD [2,3]. Beyond these two pathological hallmarks, metabolic disturbances and chronic neuroinflammation are also highly implicated in AD [4,5]. Over past decades, a broad range of drugs that singly targeting Aβ, tau or neuroinflammation have failed to halt or delay AD progression [6], implying that AD might be a systemic disease involving intricate interplay between various pathways and targets. Therefore, the therapeutic benefit of a single agent may be modest and further impeded by drug resistance mechanisms, and synergistic effects of drug combinations would be a

Abbreviations: Agpat2, 1-Acylglycerol-3-phosphate O-acyltransferase 2; Lpin3, Phosphatidic acid phosphatase 3; Aldh3b2, Aldehyde dehydrogenase 3 family member B2; Gba, Glycosylceramidase; Pla2g4a, Phospholipase a2-Iva; Pla2g6, Phospholipase A2 group VI; Lrat, Lecithin retinol acyltransferase; Gapdh, Glyceraldehyde-3-phosphate dehydrogenase; LPS, Lipopolysaccharide; Il-1β, Interleukin-1β; Il-6, Interleukin-6; Tnf-α, Tumor necrosis factor alpha.

* Corresponding authors.
E-mail addresses: zqyuan@bmi.ac.cn (Z. Yuan), huaq@bucm.edu.cn (Q. Hua), panruiyuan168@sina.com (R.-Y. Pan).

https://doi.org/10.1016/j.phrs.2022.106489
Received 18 July 2022; Received in revised form 28 September 2022; Accepted 3 October 2022
Available online 10 October 2022

better alternative for AD therapy.

Chinese medicine has a long history with multiple benefits on human health and disease and is considered as a preventive and therapeutic tool for complicated disease. The core concept of traditional Chinese medicine (TCM) theory is based on the holistic view, which can be practiced in the form of formulae. TCM formulae, namely the principle of herb compatibility, typically incorporate more than one herb. The interactions between herbs are thought to elicit synergistic effects and thus attain maximum therapeutic outcomes [7,8]. Of note, a variety of formulae have been documented to have encouraging effects on AD, including improving learning and memory, facilitating metabolism balance, enhancing central cholinergic system, promoting neurogenesis, and reducing neuroinflammation, oxidative stress, Aβ aggregation, tau hyperphosphorylation as well as neuronal apoptosis [9–14]. According to TCM theory, "phlegm" is deemed as an elementary pathogenic factor, and it is believed that the accumulation of "phlegm" in the brain drives AD pathogenesis [15,16]. Accordingly, Nao Tan Qing (NTQ), the name of which means removing phlegm from the brain in Chinese, was formulated on the basis of the TCM theory (dissipating phlegm for resuscitation). It consists of eight herbs, Dannanxing (*Arisaema Cum Bile*), Huangqin (*Scutellaria baicalensis*), Huanglian (*Coptis chinensis*), Qingbanxia (*Pinellia ternata*), Tianma (*rhizoma gastrodiae*), Ganjiang (*rhizoma zingiberis*), Shichangpu (*Acorus tatarinowii Schott*), and Zhigancao (*Radix Glycyrrhizae Preparata*).

As the era of big data and artificial intelligence approaches, the flourishing of information science provides opportunity to conduct research beyond the limitations of existing medical research methods. Systems pharmacology, including network pharmacology, molecular biology technology, metabolomics, and transcriptomics, is a powerful interdisciplinary approach combining experimental assays with computational analysis [17]. Particularly, network pharmacology has been extensively employed in TCM to uncover the molecular mechanisms underlying their efficacy [18]. A broad range of aspects of drug development strategy, such as categorizing disease, identifying and screening targets, designing clinical trial have been deeply influenced by the concept of "one drug-one target-one disease" [19]. However, the effective drugs in oncology, psychiatry, and infection fields usually function through multiple targets instead of single one [20,21]. Hence, TCM therapy and network pharmacology, both with an integrated concept, would be more desirable in AD treatment.

In the present study, using network pharmacology and experimental assays, we demonstrate that NTQ exerts strong anti-AD effects on 5×FAD mice, including amelioration of cognitive dysfunction and Aβ burden. Importantly, we find these therapeutic effects may be achieved by inhibiting neuroinflammation and regulating glycolipid metabolism.

2. Methods

2.1. Drug preparation

NTQ is comprised of Dannanxing 15 g, Huanglian 6 g, Huangqin 8 g, Qingbanxia 10 g, Tianma 10 g, Ganjiang 8 g, Shichangpu 8 g, Zhigancao 6 g, which were total 71 g and purchased from Dongzhimen Hospital (Beijing). Herbs were further prepared to be granule by Dongzhimen Hospital and kept at 4 ℃. The calculated equation is: the weight of granule (extract yield, g) / the weight of crude herbs (g). The used daily dosage of NTQ in mice is according to the clinical adult human daily prescription amount: (71 g raw herbs / 70 kg body weigh) * 9.1 *extract yield (0.025).

2.2. Animal and drug administration

5×FAD mice used in this study have been described previously [22]. All mice were maintained at 22 ℃ and a 12 h circadian rhythm. All experimental animal procedures were approved by the Institution of Animal Care and Use Committee of the Beijing Institute of Basic Medical Sciences (Beijing, China).

48 5×FAD mice were randomly divided into four groups: 5×FAD, 5×FAD + NTQ (0. 25 g/kg), 5×FAD + NTQ (2.5 g/kg) and 5×FAD + memantine (10 mg/kg) group, 12 mice per group. The drug was administered to mice at 75 days of age for 90 consecutive days by gavage at 0.1 mL/10 g dosing volume. Another 12 wild type (WT) littermates were given the same volume of ddH_2O as control.

2.3. Genotype identification

Mice were labeled with foot numbers from birth to 2–3 weeks, and the cut mouse toes were added to 200 μL of mouse tail lysate (containing proteinase K 50 μg/mL) and kept overnight at 55 ℃. centrifuge at 18,000g for 10 min, then collect the supernatant, add isopropanol of the same volume, and mix it upside down. 18,000g at 4 ℃ for 10 min again and remove the supernatant. The DNA precipitate was washed once with 75% ethanol, dried and then added 60–80 μL of ddH_2O to fully dissolve it for genotype identification by PCR. The primers for mouse genotype identification: upstream: AATAGAGAACGGCAGGAGCA. downstream: GCCATGAGGGCACTAATCAT. 94 ℃ maintained 3 min; 94 °C 30 s; 54 °C maintained 1 min; 72 °C maintained 1 min; 35 cycle; 72 °C maintained 3 min; 4 °C ∞.

2.4. Behavior test

2.4.1. Morris water maze

Maze consists of a circular pool, a circular platform that can just accommodate the mice, and a camera video acquisition system above. The pool is filled with water and the temperature is maintained at 22 °C + 1.0 °C. platform is submerged 1 cm below the water surface and water was rendered opaque by adding titanium dioxide. The water depth was 60 cm, and the edges were set with four starting points for mice to enter the water, east, south, west and north, respectively. Different colored and shaped objects were attached to the walls to provide visual cues for mice spatial orientation. As they enter the maze and find the platform more often, normal mice will find the platform more effectively and more quickly to exit the maze. The time it took for the mice to find the platform was recorded and defined as the escape latency. The water maze experiment was divided into a 6-day training period and a 1-day exploration period. Mice were trained twice a day. If the mice could not find the platform within 60 s, they were guided to the platform and left for 30 s to learn and remember the platform location. 24 h after the end of the mice training, the probe test was performed. The platform was removed but the position of the platform was recorded, and the mice were also placed in the water facing the wall of the pool and allowed to swim freely for 60 s before being rescued. The number of times the mice crossed the platform during the swim and the time spent in the platform quadrant were recorded.

2.4.2. New object recognition (NOR) experiment

NOR, an important method for testing cognitive function of rodents, is based on the principle of exploiting the natural preference of mice for novelty. It consists of a 50 × 50 × 20 cm rectangular apparatus and takes 4 days. Days 1–3 are the adaption period and each mouse was placed in an empty rectangular box and allowed to explore freely for 5 min, at the end of which the mice were taken out and the box was wiped with 75% ethanol to remove the odor before the next trial. On the fourth day, two identical objects were placed in the rectangular box and fixed with double-sided tape, and the mice were placed in the device to freely explore for 5 min, after which the mice were taken out and the box was wiped with 75% ethanol to remove the odor.

1 h later, replace one of the objects with a new object, and put the mice back into the device, free to explore the 5 min. The time spent by the mice exploring each object was recorded with a video camera mounted overhead and was automatically monitored by ANY-maze behavioral tracking software (Stoelting, Wood Dale, IL, USA).

2.5. Immunofluorescence

After the 4% PFA-fixed brain tissue was dehydrated with 30% sucrose, the brain was cut into 40 μm coronal sections by frozen sectioning machine (CM3050S, Leica) and the brain sections were then placed in 1 × PBS. For long term storage, PBS was replaced with antifreeze solution (5 mM Na2HPO4, 30% sucrose, 20 mM NaH2PO4, 30% ethylene glycol and 1% polyvinyl-pyrrolidone) and stored at − 20 ℃ [23]. After three times washes with PBS, 3% hydrogen peroxide was incubated for 15 min to inhibit endogenous peroxidases. Then, the sections were washed three times with PBS and blocked for 1.5 h with blocking buffer (PBS containing 0.3% TritonX-100, 5% goat serum and 2% BSA) at room temperature, followed by primary antibodies overnight at 4 °C. Primary antibodies used include rabbit polyclonal anti-Iba1 (019–19741, Wako, Richmond, VA, USA) and mouse monoclonal anti-GFAP (MAB360, Millipore, Darmstadt, Germany). Next day, the sections were labeled with fluorescent secondary antibodies [TRITC AffiniPure goat anti-rabbit IgG (111–025–003, Jackson ImmunoResearch) and Cy5-conjugated donkey anti-mouse IgG (715–175–150, Jackson ImmunoResearch)]. The images were acquired using a Nikon confocal microscope (Nikon, Melville, NY, USA).

2.6. Thioflavin S staining

Thioflavin S (TS) allows the visualization of amyloid plaques. Brain sections were stained with 0.002% TS (dissolved in 50% ethanol) for 8 min, washed twice with 50% ethanol and 3 times with PBS. After blocking, brain sections were incubated with other antibodies for subsequent immunofluorescence staining or were mounted for imaging.

2.7. BV2 Cell culture and drug treatment

The immortalized murine microglial BV2 cell line was purchased from the Cell Resource Center, Institute of Basic Medical Science, Peking Union Medical University and cultured in DMEM containing 10% heat-inactivated fetal bovine serum and 1% penicillin/streptomycin (Sigma-Aldrich).

BV2 cells were plated in 24–well culture plates at a density of 5 × 10^4cells/well. After 6 h incubation, the cells were pretreated with 20 μM of chemical compounds respectively [Apigenin (Selleck, NO. S2262), Berberine (Selleck, NO. S9046), Baicalein (Selleck, NO. S2268) and Calycosin (Selleck, NO. S9038)] for 0.5 h, followed by stimulation with 1 μg/mL LPS for 3 h or 6 h. Following treatment, the cultured medium was removed, and the cells were washed three times with PBS and collected for RNA extraction and examination.

2.8. Gene silencing assay

BV2 cells in 24-well plates containing about 1 × 10^5 cells per well were transfected with a 50 μL mixture containing 50 nM small interfering RNA (siRNA), 2 μL Lipofectamine RNAiMAX (Thermo Fisher), Opti-MEM (Invitrogen). siRNA sequences used are listed as follows: *Lpin3: CCCAGAGAGUAAGGAAACCAA. Agpat2: GGUUCGUUCGGUCCUUCAATT. Lpin3* and *Agpat2* assays were performed at 50–72 h after transfection.

2.9. Real-time quantitative polymerase chain reaction (qPCR)

Total RNA from tissues or cells was extracted using Trizol reagent (Invitrogen), followed by cDNA synthesis with a One-step First-strand cDNA synthesis kit (Transgen). Quantitative analysis of the expression of *Il-1β*, *Il-6*, *Tnf-α*, *Agpat2*, *Lpin3* and *β-actin* was performed using RT-PCR with 96–well optical reaction plates using the Quant-Studio qPCR System. The primer sequences for qPCR are listed in Table 1. The mRNA expression levels were normalized to that of β-actin.

2.10. Identification of chemical composition of NTQ

Reagents: methanol and acetonitrile at LC-MS level were purchased from Merck.

The NTQ granule were powdered; for every 100 mg of NTQ powder, 1.2 mL of 70% methanol extract was used for dissolution; after that, the solution was vortexed every 30 min for a total of 6 times and then stored at 4 °C; the supernatant was collected by centrifugation at 18,000g for 10 min the next day. supernatant was filtered using a microporous membrane (0.22 μm) and then stored in an injection vial. The sample preparation was completed, pending subsequent UPLC-MS/MS analysis.

Serum sample preparation and extraction after oral administration of NTQ.

Take out the sample from the − 80 °C refrigerator and thaw it on ice, vortex for 10 s to mix well. Take 50 μL of the sample and put it into a 1.5 mL centrifuge tube. Add 300 μL of 70% methanol internal standard extract, vortex for 3 min, centrifuge for 10 min at 18,000g, 4 °C. Pipette 200 μL supernatant and put it into another 1.5 mL centrifuge tube, after standing in the − 20 °C refrigerator for 30 min, centrifuge again for 3 min at 18,000g, 4 °C. Pipette 180 μL supernatant and store it in an injection bottle for UPLC-MS/MS detection.

An Agilent SB-C18 column of 1.8 μm × 2.1 mm× 100 mm was used as the liquid phase and maintained at 40 °C. The injection volume was 4 μL and the flow rate was set at 0.35 mL/min. The mobile phases were ultrapure water with 0.1% formic acid and acetonitrile with 0.1% formic acid as the A and B phase, respectively. The elution gradient was set to start with a B-phase ratio of 5%, which increased linearly to 95% over the next 9 min and was maintained until 10 min, and then decreased to 5% over the next minute and was maintained until 14 min

Mass spectrometry: LIT and QQQ scans were carried out in Q TRAP UPLC-MS/MS system. Source temperature was set at 150 °C; the negative and positive ion IS modes were − 4500 V, and 5500 V, respectively; GSI, GSII and CUR were 50, 60 and 25.0 psi, respectively, collision-induced ionization was adjusted to the high setting. Calibrations of the apparatus were performed using polypropylene glycol solution with different concentrations of 100 and 10 μM in LIT and QQQ modes, respectively. The QQQ scan is in the MRM mode with the collision gas being set to medium. based on the metabolites that are eluting during each period, defined set of MRM ion matches is detected.

Substance characterization is developed from the Metware database and is based on secondary spectral data. Some signals need to be removed during the analysis, such as duplicate signals containing K^+, Na^+, $NH4^+$ ions, isotopic signals, *etc.*

Table 1
The list of qPCR primers.

Gene target	Forward sequence	Reverse sequence
β-actin	GGCTGTATTCCCCTCCATCG	CCAGTTGGTAACAATGCCATGT
Il-1β	TGTAATGAAAGACGGCACACC	TCTTCTTTGGGTATTGCTTGG
Tnf-α	CAGGCGGTGCCTATGTCTC	CGATCACCCCGAAGTTCAGTAG
Il-6	GCTACCAAACTGGATATAATCAGG	CCAGGTAGCTATGGTACTCCAGAA
Agpat2	CAGCCAGGTTCTACGCCAAG	TGATGCTCATGTTATCCACGGT
Lpin3	CAAACCTCGTGGTGAAAATCAAC	CCACAGTGCTCTCAGGTAAGT

2.11. Metabolomics

First, 500 μL of extract solution was prepared by mixing methanol and acetonitrile in one-to-one volume and adding internal marker to get a concentration of 2 mg/L. 100 μL of serum sample was added, and then mixture was vortexed and ultrasound homogenized in an ice-water bath, and left to stand for 1 h at − 20 °C; then centrifuged again at 18,000g for 15 min; 500 μL of supernatant was collected and dried, and then 160 μL was used again. The supernatant was collected for drying. The sample was then dissolved again with 160 μL of extraction solution; the vortex and centrifugation step were repeated. At the end of the procedure, 120 μL of supernatant was put into a 2 mL injection vial, and 10 μL of each sample was mixed for further operation.

The sample volume was 1 μL. The mobile phases A and B were adjusted to 0.1% formic acid pure water and 0.1% formic acid acetonitrile in positive ionization mode. In the negative ionization mode, the mobile phases A and B were adjusted to 0.1% formic acid pure water and 0.1% formic acid acetonitrile, respectively. (Table 2).

The mass spectrometer was Xevo G2-XS QT of Dual channel data acquisition was performed in MSe mode using MassLynx V4.2, Waters software at low collision energies (2 V) and high collision energies (10–40 V). The mass spectra were scanned every 0.2 s. The positive and negative ion modes were 2000 V and − 1500 V, respectively; the cone hole voltage was set to 30 V; ion source temperature was 150 °C; the desolvation gas temperature was 500 °C; the blowback gas flow rate was set to 50 L/h; and the desolvation gas flow rate was set to 800 L/h.

For the analysis of the data, the peak of obtained data was first extracted and aligned by Progenesis QI software. The identification and theoretical fragmentation were performed using the online METLIN database and Biomark's own library to keep the mass number deviation within 100 ppm. The data were processed using unit-variance scaling and partial least squares-discriminant analysis (PLS-DA). Finally, with SPPS, t-test was used to compare the two groups of data. Setting variable importance, VIP $>$ 1 and P $<$ 0.05 were used as thresholds to obtain significantly different metabolites. Heatmap in R language was then used for graphing. Pathway analysis of differential metabolites was then performed by MetaboAnalyst 5.0, and compound-response-protein-gene interaction networks were constructed and visualized by the MetScape plugin in Cytoscape.

2.12. Transcriptomics

Total RNA from mice hippocampal tissues were purified by TRIzol (Invitrogen), and verified by quality control and integrity testing using ND-1000 (NanoDrop) and Bioanalyzer 2100 (Agilent), agarose electrophoresis. RNA needs to meet concentration $>$ 50 ng/μL, RIN value $>$ 7.0, OD260/280 $>$ 1.8, total RNA $>$ 1 μg RNA purification: mRNA with polyadenylates was trapped by magnetic beads (Thermo Fisher) and fragmented by Magnesium RNA Fragmentation Module; cDNA was next synthesized using reverse transcriptase (Invitrogen). E. coli DNA polymerase I with RNase H were used to convert the complex duplex of DNA and RNA into a DNA duplex while dUTP Solution was mixed into the duplex to complement the ends of the double-stranded DNA to flat ends. Then an A base was added at each end to ligate with a connector with a T base at the end, and the fragment size was screened and purified using magnetic beads.

The second strand was digested using UDG enzyme and predenatured for PCR by holding at 95 °C for 3 min, denaturing at 98 °C for 8 cycles of 15 s each, annealing to 60 °C for 15 s, extending at 72 °C for 30 s, and holding at 72 °C for 5 min to make a library with a fragment size of 300 bp ± 50 bp. Finally, it was double-end sequenced using illumina Novaseq™ 6000 in PE150 sequencing mode. For data analysis, the raw data were processed using cutadapt-1.9 software to remove splice low quality sequences and duplicate sequences to obtain CleanData in the format fastq.gz. The new data were compared to the genome using HISAT2–2.0.4 and the bam files were obtained. The initial assembly was performed using StringTie software and merged, and the final assembly annotation results were obtained by checking the comparison of transcripts with the reference annotation using gffcompare software. FPKM quantification [FPKM = total_exon_fragments / mapped_reads (millions) × exon_length (kB)] was performed using the ballgown package to provide file input with the parameters ~stringtie -e -B -p 4 -G merged.gtf -o samples.gtf samples.bam. Use the R package edgeR (https://bioconductor.org/packages/release/bioc/html/edgeR.html) or the R package DESeq20 (http://www. bioconductor.org/packages/release/bioc/html/DESeq2.html) Significant difference analysis was performed between samples, and genes with Fold Change $\geq$ 1 and P $<$ 0.05 were defined as differential genes and subjected to GO (Gene Ontology) and KEGG (Kyoto Encyclopedia of Genes and Genomes) enrichment analysis. Passage integration analysis was obtained using the (Transcriptome-based Multi-scale Network Pharmacological Platform) TMNP website.

Table 2
Liquid chromatography gradient parameters.

Time (min)	Flow rate (μL/min)	A%	B%
0.0	400	98	2
0.25	400	98	2
10.0	400	2	98
13.0	400	2	98
13.1	400	98	2
15.0	400	98	2

2.13. Statistical analysis

SPSS 24.0 was used for data statistics. For measurement data, two-tailed t-test was used for comparison of two groups; for multiple group comparisons, chi-square test was performed followed by one-way or two-way analysis of variance (ANOVA). Statistically significant difference scale was set at 0.05; P $<$ 0.05 indicated that the hypothesis test was statistically significant and there was a significant difference in the comparison; P $<$ 0.01, P $<$ 0.001 and P $<$ 0.0001 indicated that the hypothesis test was statistically significant and there was a highly significant difference.

3. Results

3.1. NTQ rescued cognitive impairment of 5×FAD mice

To test protective effect of NTQ on AD, 2.5-month-old 5×FAD mice were orally administered with NTQ (5 g/kg/day or 50 g/kg/day) or memantine (10 mg/kg/day, used as positive control) orally for 4 months, followed by behavioral tests and pathological analyses (Fig. 1A). The body weight of the mice was not significantly different among groups, suggesting no obvious side effect of NTQ within the selected concentration (Fig. 1B). A Morris water maze test showed that during training days, the mean escape latency was significantly longer in the 5×FAD mice than that in wild type (WT) mice. In contrast, the mean escape latency of mice treated with NTQ or memantine group was significantly shorter than 5×FAD mice (Fig. 1C). In the probe trial, mice in the NTQ or memantine group crossed the platform more times and stayed in the target quadrant longer than 5×FAD mice (Fig. 1D, E). These data suggest that NTQ significantly improve spatial learning and memory in 5×FAD mice. Notably, no significant difference was observed in the swimming speed of the mice among five groups (Fig. 1F), indicating that the ameliorative effects of NTQ did not result from altered motor ability.

Additionally, a novel object recognition (NOR) test was performed to examine the cognitive ability of mice. The results showed that 5×FAD model mice had no significant preference to the novel object, while 5×FAD mice treated with NTQ or memantine group had more chatting

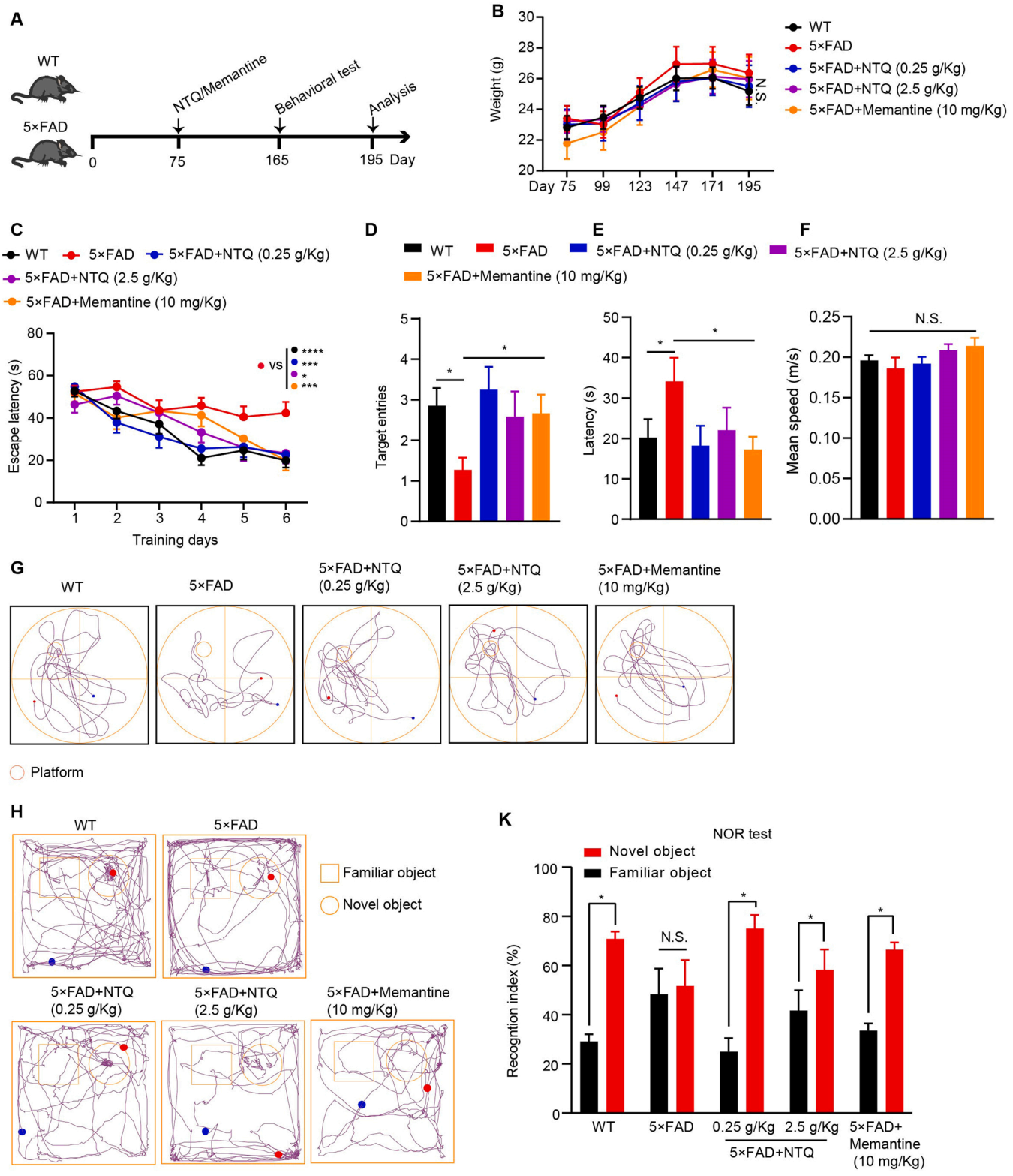

Fig. 1. NTQ improves cognitive function in 5×FAD mice. (A) Experiment timeline. (B) Body weight difference. (C) Escape latency during training days in Morris water maze. (D) Numbers of target cross in the probe test. (E) Time stayed in target quadrant in the probe test. (F) Average swimming speeds of mice (G) Representative track images of mice during probe test (Morris water maze test). (H) Representative track images of mice in the probe test (Novel object recognition test). (K) Quantification of the chatting time in novel object recognition test (n = 12 mice per group). Data are mean ± SEM. *P < 0.05, * **P < 0.001, * ** *P < 0.0001, N.S. no significant difference, two-way ANOVA, followed by Tukey's multiple comparisons test (B and C) or one-way (D, E and F) or Two-tailed unpaired Student's t test (K).

time on the novel object, which was similar to those in the WT mice (Fig. 1K). Together, these behavioral tests suggest that NTQ could restore the cognitive decline in AD mice.

3.2. NTQ reduced Aβ burden in the brains of 5×FAD mice

Aβ plaque is an important pathological hallmark of AD and evidence shows that robust plaque deposition begins at 2–3 months of age in the brains of 5×FAD mice [24]. To examine whether NTQ treatment affect the Aβ deposition in 5×FAD mice, we next performed Thioflavin S (TS) staining. The results showed that TS-positive Aβ plaques in brain regions, including the cortex and the hippocampus, were significantly decreased in 5×FAD mice administrated with NTQ or memantine compared with 5×FAD control mice (Fig. 2A-E), suggesting that NTQ could reduce Aβ burden in the brains of 5×FAD mice.

3.3. NTQ suppressed glial activation in 5×FAD mice

Chronic neuroinflammation with aberrant activation of glial cells has been demonstrated to be a pathological feature of AD [25,26]. We next detected whether NTQ could prevent the activation of glial cells. Brain sections were first incubated in TS solution and then labeled with specific markers for astrocyte and microglia with antibodies against GFAP and Iba1, respectively [27]. As expected, abnormal activation of microglia and astrocytes were observed in brain regions of 5×FAD mice compared with the WT mice, as indicated with enlarged cell bodies and gliosis, including in brain regions of hippocampal dentate gyrus (DG) and prefrontal cortex (PFC) (Fig. 3A, B). However, these glial activation phenotypes were significantly suppressed in the NTQ or memantine treated 5×FAD mice compared with the 5×FAD control mice (Fig. 4C-F), indicating that NTQ could inhibit neuroinflammation in AD mice.

3.4. Identification of chemical composition of NTQ

To analyze the effective chemical composition of NTQ, UPLC-MS/MS was performed (Fig. 4A). The results displayed 906 peaks, each representing one compounds, including 226 Flavonoids, 151 Phenolic acids, 88 Alkaloids, 87 Organic acids, 69 Amino acids and derivatives, 45 Lipids, and other types of compounds (Supplementary Table S1). Then, we performed UPLC-MS/MS to investigate phytochemistry ingredients of NTQ and their absorption in mice serum from the mice after 1 h of oral administration of NTQ. To analyze the effective chemical composition of NTQ, the results displayed 175 phytochemistry ingredients in mice serum after oral administration of NTQ. Combine the results of these detections,74 was identified from NTQ based on literatures and database for network pharmacology analysis [28,29]. The detailed chemical compounds are listed (Supplementary Table S2).

3.5. Network pharmacology uncovered the targets and signaling pathways regulated by NTQ

Based on the 74 active ingredients of NTQ, the corresponding targets were searched using the SymMap database (Supplementary Table S3). KEGG pathway enrichment and correlation network diagram were constructed for the targets of related Chinese medicine components. As seen from the diagram, the top 20 pathways mainly involved metabolic and inflammation-related pathways, which included PI3K-Akt, AGE-RAGE, and HIF-1 signaling pathway (Fig. 4B). These results suggest that

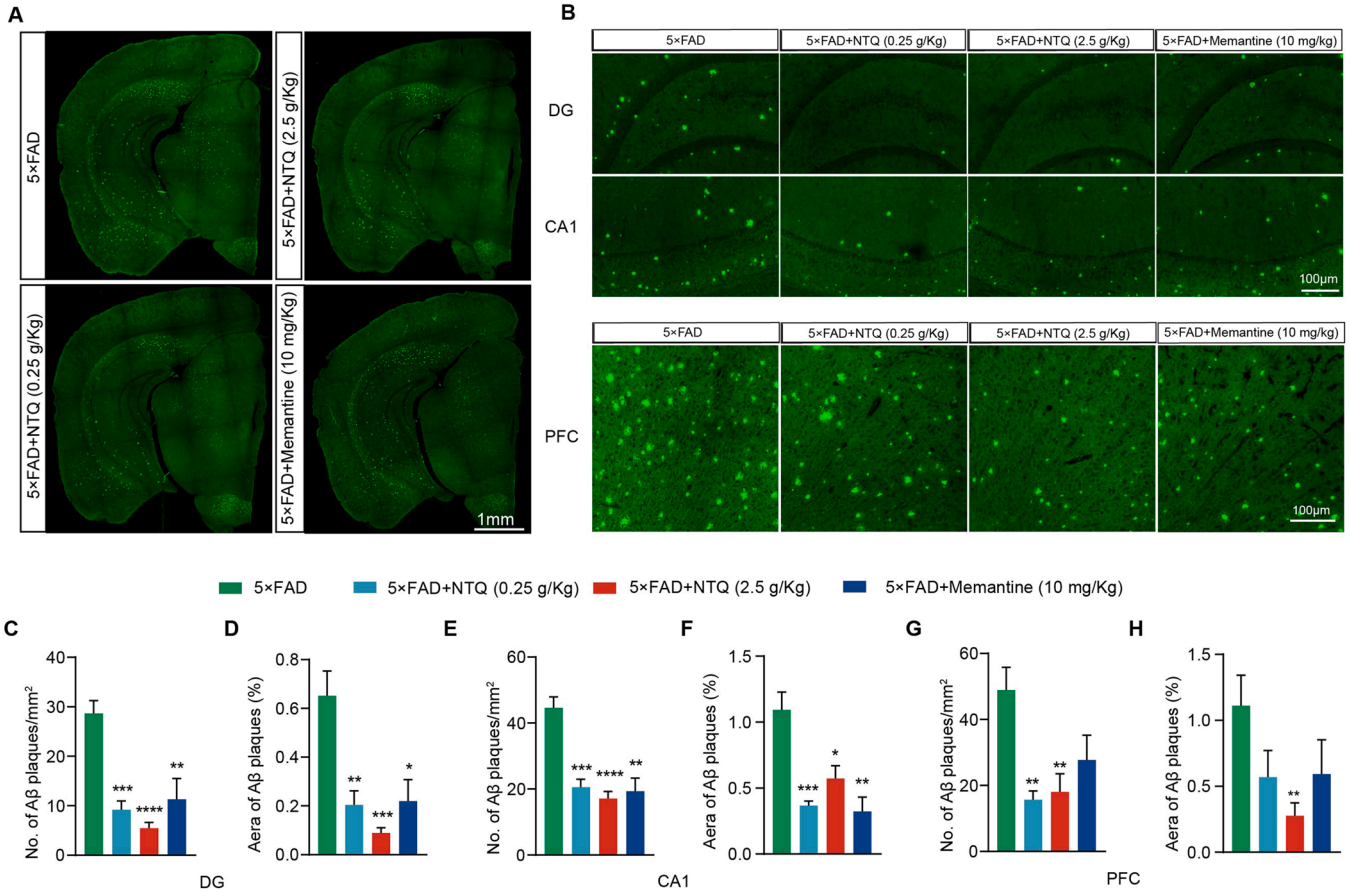

Fig. 2. NTQ alleviates Aβ burden in 5×FAD mice. (A) Representative images of TS staining. (B) Enlarged images of TS staining in indicated brain regions. (C-H) Quantification of the Aβ plaques (n = 5–10 brain sections, from three mice per group) in the hippocampal DG and CA1 regions, and the cortex from indicated group mice. Data are mean ± SEM. * , P < 0.05; * *, P < 0.01; * ** , P < 0.001; * ** *, P < 0.0001, one-way ANOVA, followed by Tukey's multiple comparisons test.

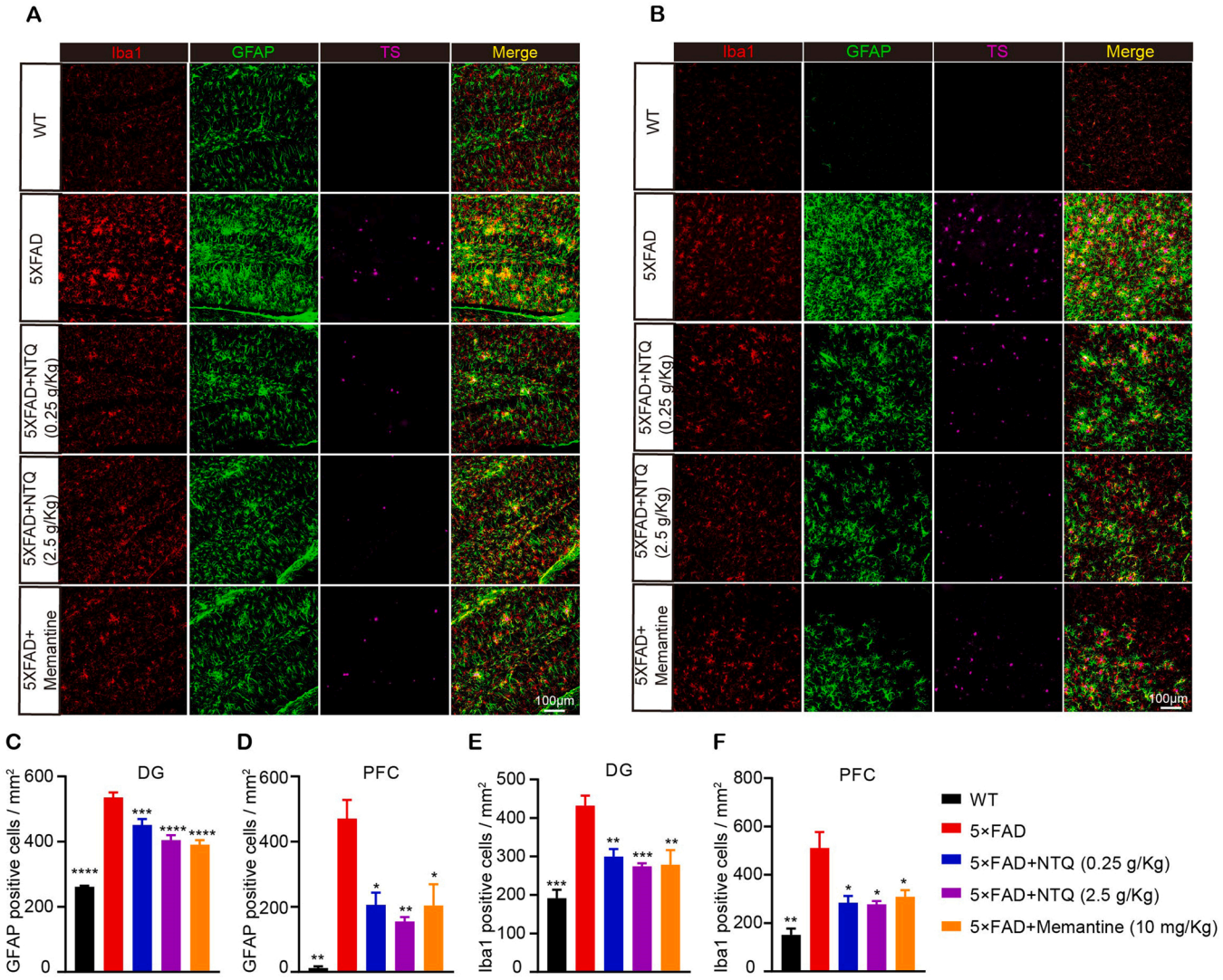

Fig. 3. NTQ suppresses gliosis in 5×FAD mice. (A, B) Representative images of Aβ plaques (TS), microglia (Iba1), and astrocyte (GFAP) in the hippocampal DG region (A) and the PFC (B) from indicated group mice. (C, D) Quantification of Iba1positive microglia in the hippocampal DG region (C) and the PFC (D) from indicated group mice (n = 5–10 brain sections from three mice per group). (E, F) Quantification of GFAP positive astrocytes in the hippocampal DG region (E) and the PFC (F) from indicated group mice (n = 5–10 brain sections from three mice per group). Data are mean ± SEM. * , $P < 0.05$; * *, $P < 0.01$; * ** , $P < 0.001$; * ** *, $P < 0.0001$, one-way ANOVA, followed by Tukey's multiple comparisons test.

NTQ might exert protective effects against AD through regulating signaling pathways associated with neuroinflammation and metabolism.

To confirm our hypothesis, we constructed a drug-target-disease-pathway network analysis based on the correlation analysis between the targets of drug action and AD targets. The results showed that the main active ingredients of NTQ acting on AD were baicalein, berberine, apigenin and calycosin, and mainly targeted AD pathology-related pathways including Aβ binding, lipid metabolism pathway, PI3K-Akt, AGE-RAGE and HIF-1 signaling pathway, *etc.* (Fig. 4C). These data confirm that NTQ can target neuroinflammation and glycolipid metabolism for protecting against AD.

3.6. NTQ regulated inflammatory and metabolic pathways in hippocampus of 5×FAD mice

To determine the biological factors and signaling pathways associated with the efficacy of NTQ, RNA-sequencing on hippocampus was performed. By applying the cutoffs of $P < 0.05$ and log2 Fold Change > 0, 149 differentially expressed genes were identified, among which 42 genes were upregulated whereas 107 genes were downregulated (Fig. 5A, B). These genes were further organized into functional pathways, and over 100 KEGG biological processes were identified to be enriched (Supplementary Fig. S4). Top 20 ranking pathways included amoebiasis, inflammatory bowel disease, glycerolipid metabolism pathways, focal adhesion, relaxin signaling pathway, estrogen signaling pathway, protein digestion and absorption, ferroptosis, and glycerophospholipid metabolism (Fig. 5D). Additionally, we observed that lipid metabolism-associated genes such as *Aldh3b2*, *Agpat2* and *Lpin3* were hub DEGs (differentially expressed genes) (Fig. 5C).

The correlation of NCS (Normalized correlation score) values at the pathway scale ($R = -0.76$) showed that the differential genes in NTQ-treated mice were negatively correlated with the associated differential genes in the 5×FAD control mice (Fig. 5E). Consistently, the heat mapping of NCS values confirmed these observations (Fig. 5F). We next focused on the detailed features and found that over 100 pathways were regulated by NTQ. Toll-like receptor and NF-kappa B signaling, Pentose and glucuronate interconversions, and Oxidative phosphorylation pathway were remarkably enriched after NTQ treatment (Fig. 5 G).

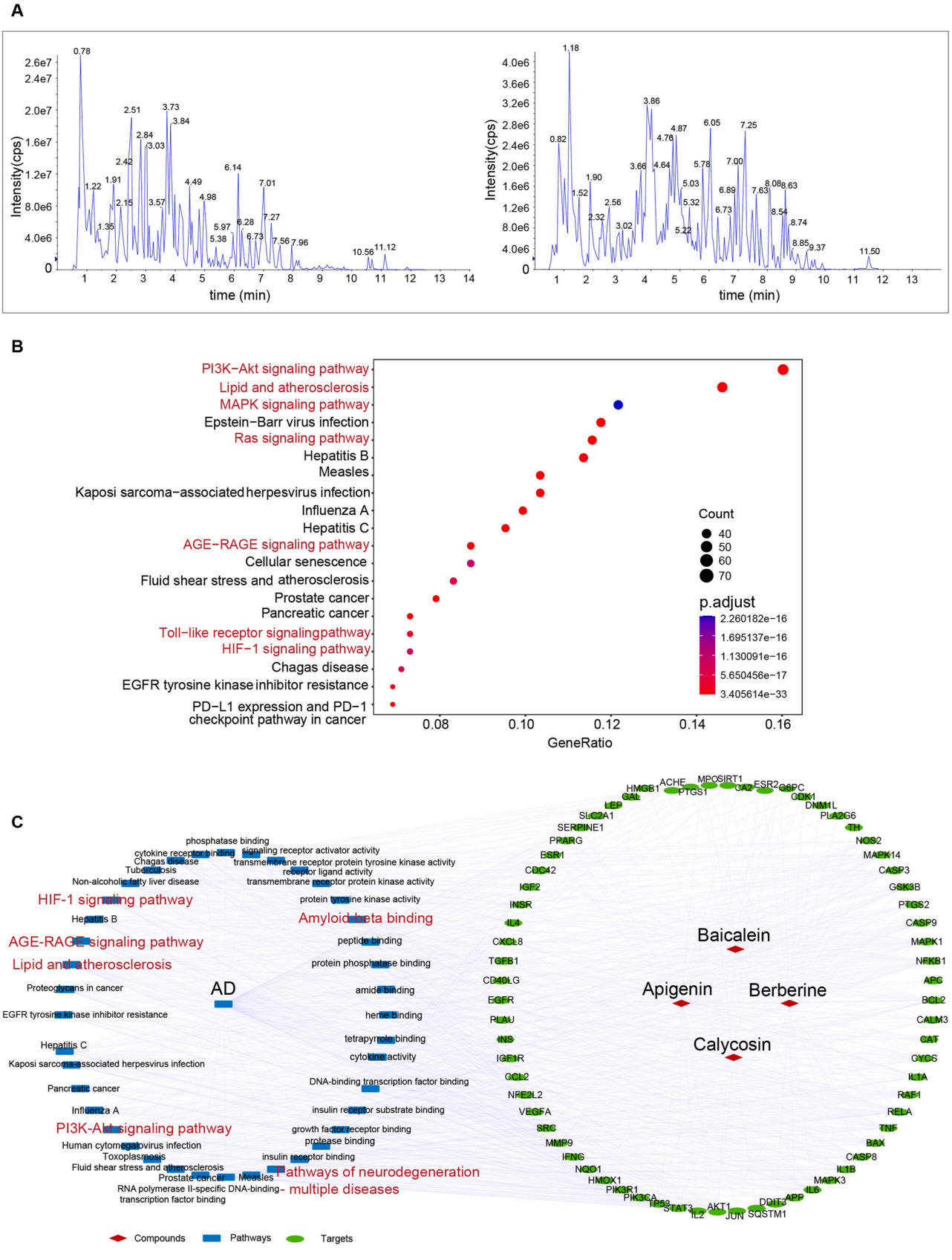

Fig. 4. Network pharmacology analysis revealed the targets and pathways regulated by NTQ in AD. (A) Mass spectrum chromatograms of NTQ (Negative mode and Positive mode). (B) KEGG enrichment analysis showing the signaling pathways that regulated by NTQ. (C) Target-pathway-disease network of the main components of NTQ from drug-target-disease-pathway network analysis based on the correlation analysis between the targets of drug action and AD targets.

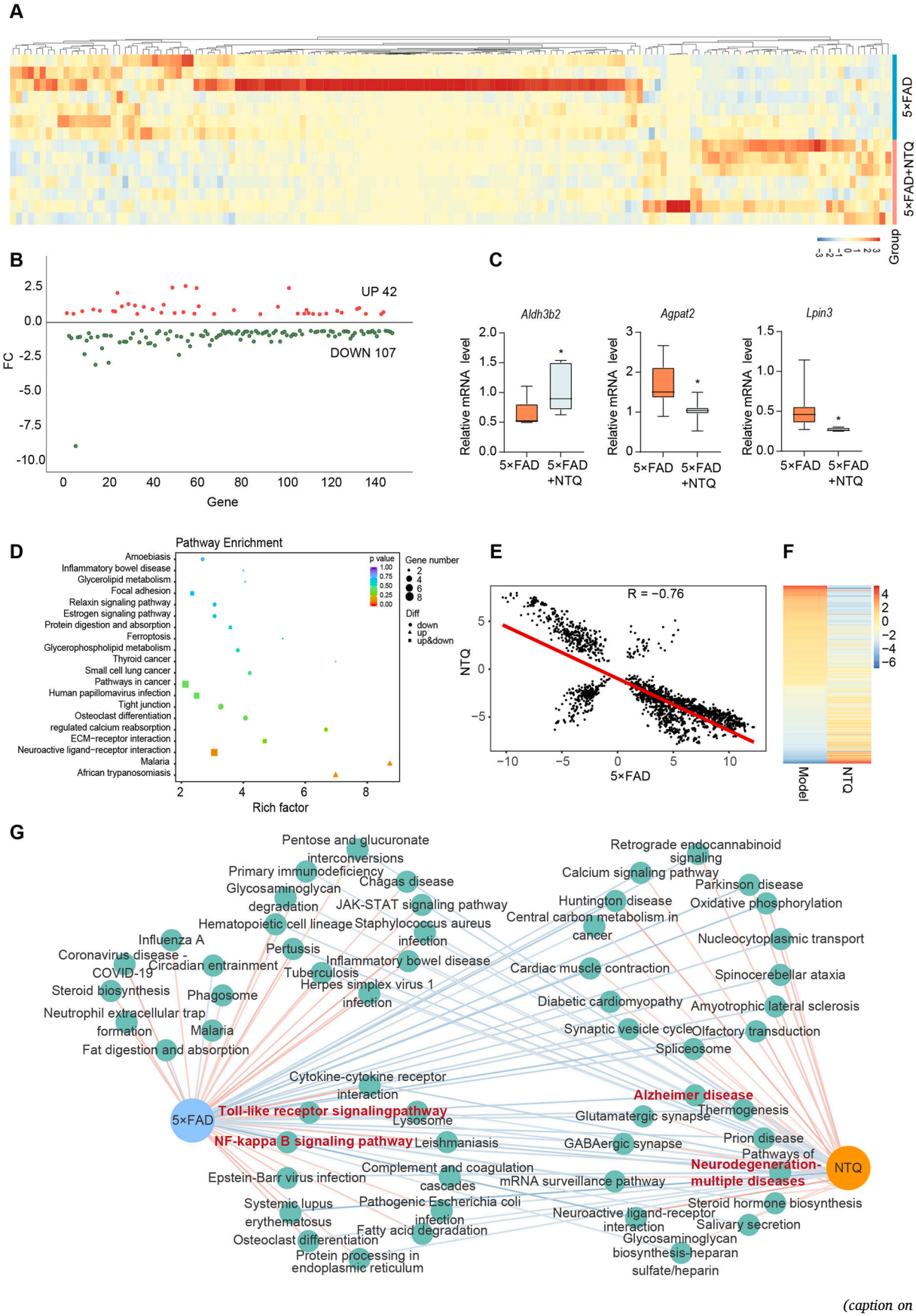

(caption on next page)

Fig. 5. Transcriptomics analysis of hippocampus from 5×FAD mice. (A) The heat maps of differentially expressed genes (DEGs) between 5×FAD and 5×FAD+NTQ mice. Red denotes higher expression level, while blue denotes lower expression level. (B) P value < 0.05, Fold Change (FC) of DEGs in NTQ-treated 5×FAD mice *vs.* 5×FAD control mice. (C) Glycerol phospholipid metabolism related DEGs level in NTQ-treated 5×FAD mice *vs.* 5×FAD control mice (n = 7 per group. *, P < 0.05, Two-tailed unpaired Student's t test). Whiskers indicates min to max, and horizontal line indicates the median. (D) KEGG enrichment analysis of DEGs in NTQ-treated 5×FAD mice *vs.* 5×FAD control mice. (E, F) Pathway-based correlation analysis. The correlation of NCS (Normalized correlation score) values at the pathway scale in 5×FAD control mice *vs.* WT mice and NTQ-treated 5×FAD mice *vs.* 5×FAD control mice. (G) The NTQ pathway association network. The link between NTQ (or 5×FAD) and one pathway indicates that the pathway is significantly regulated (FDR < 0.05). The red and blue lines represent NCS > 0 and NCS < 0, respectively. In the network, the incorporated pathways are significantly related to NTQ.

3.7. NTQ remodeled metabolic profiling of 5×FAD mice

To further explore the potential mechanisms accounting for the protective effects of NTQ against AD, we conducted serum untargeted metabolomics. OPLS-DA score plots of NTQ-treated 5×FAD mice were obviously distinguished from that of 5×FAD control mice. The cumulative values of R2X, R2Y and Q2Y indicated that the method has good predictive and interpretative capacity (Fig. 6A). 140 variable metabolites were identified with (Variable important in projection) VIP > 1 and p < 0.05 between NTQ treated 5×FAD mice and 5×FAD control mice (Fig. 6B). To obtain functional information about the differential metabolites, the KEGG database was applied. The results were verified by standard products and 40 metabolites were identified (Fig. 6C).

MetaboAnalyst software was applied to analyze differential metabolic pathways. Results showed that pathways associated with glucose and lipid metabolism were markedly changed after NTQ treatment, including fructose and mannose metabolism, pentose phosphate pathway, glycerophospholipid metabolism, sphingolipid metabolism, and glycolysis/gluconeogenesis (Fig. 6D). Based on pathway impact value, we found that fructose and mannose metabolism as well as pentose phosphate pathway were the most significantly enriched pathways in NTQ group (Fig. 6E). Additionally, we established an interaction network based on differential metabolites: Cytoscape's MetScape was used to obtain compound-reaction-enzyme-gene networks from metabolites, and the results screened out five key targets of AD, *Gba*, *Pla2g4a*, *Pla2g6*, *Lrat*, and *Gapdh* (Fig. 6F).

Taken together, both the transcriptomics and metabolomics reveal that NTQ might protect against AD pathology through regulating neuroinflammation and glycolipid metabolism pathways.

3.8. NTQ reduced the levels of pro-inflammatory factors

To experimentally demonstrate the omics data that NTQ exerted anti-AD property by regulating neuroinflammation and metabolism, we performed qPCR analysis to evaluate the pro-inflammatory factors in hippocampus (Fig. 7A). The results showed that the levels of pro-inflammatory factors including *Il-1β*, *Il-6* and *Tnf-α* were significantly increased in 5×FAD mice compared to the WT mice, whereas NTQ treatment markedly down-regulated these pro-inflammatory factors in 5×FAD mice (Fig. 7B-D). Additionally, we evaluated the anti-inflammatory effects of NTQ active compounds (calycosin, apigenin, berberine and baicalein) on cultured microglial BV2 cells. Consistent with the *in vivo* results, we found that four tested compounds of NTQ (calycosin, apigenin, berberine and baicalein) significantly suppressed the inflammatory responses of BV2 cells stimulated by LPS, as indicated by significant decrease of *Il-1β*, *Il-6* and *Tnf-α* levels (Fig. 7E-G). These *in vivo* and *in vitro* results demonstrate that NTQ can inhibit neuroinflammation.

3.9. NTQ inhibited neuroinflammation via regulating glycolipid metabolism

We next experimentally confirmed the effects of NTQ on glycolipid metabolism in 5×FAD mice. Of note, transcriptomic data revealed that *Lpin3* and *Agpat2* were the most hub DEGs in the glycerophospholipid metabolic pathway (Fig. 5C). In agreement with these omics, our qPCR analysis showed that the mRNA levels of *Lpin3* and *Agpat2* were significantly increased in 5×FAD mice compared to the WT mice. In contrast, we found that NTQ treatment dramatically down-regulated *Lpin3* and *Agpat2* levels in 5×FAD mice (Fig. 8A, B). To clarify the hierarchy of neuroinflammation and glycolipid metabolism pathways regulated by NTQ, we performed experiments with siRNA to knockdown *Lpin3* and *Agpat2*, followed by examining the effects of NTQ ingredients on cytokines in LPS (lipopolysaccharide)-stimulated BV2 cells. As expected, the mRNA levels of *Agpat2* and *Lpin3* were significantly down-regulated in indicated siRNA transfected BV2 cells compared to the NC (scramble siRNA sequence) cells, indicating efficient knockdown strategy (Fig. 8C, D).

Next, we investigated the levels of pro-inflammatory factors (including *Il-1β*, *Il-6* and *Tnf-α*) in LPS-stimulated BV2 cells after *Agpat2* and *Lpin3* knockdown in the presence or absence of NTQ ingredients (*Calycosin*, *Apigenin*, *Berberine* and *Baicalein*). As expected, we found that each of these ingredients exerted significant anti-inflammatory responses properties, as evidenced by dramatic decrease of pro-inflammatory factors (*Il-1β*, *Il-6* and *Tnf-α*) in LPS-stimulated BV2 cells. Interestingly, we found that there was a significant reduction in the levels of these pro-inflammatory factors in *Agpat2* and *Lpin3* knockdown BV2 cells compared to the control cells. Of note, the anti-inflammatory effects of some NTQ ingredients were partially attenuated in *Agpat2* and *lpin3* knockdown BV2 cells compared to the control cells (Fig. 8E-G), indicating that NTQ might inhibit inflammation through down-regulating the expression of *Agpat2* and *Lpin3*. Indeed, we found that all the tested NTQ ingredients could significantly reduce the mRNA levels of *Agpat2* and *Lpin3* in BV2 cells (Fig. 8H, I). Collectively, these results suggest that NTQ might exert anti-neuroinflammation through regulating glycolipid metabolism.

4. Discussion

Over the past decades, despite there were a few pharmacological approaches for AD advanced clinical development, none have achieved satisfactory results [30]. Therefore, pursuit of novel effective drugs and/or strategies for AD is still an urgent need. In the long-term clinical practice, TCM has accumulated a large number of effective prescription drugs under the guidance of holistic view and dialectical treatment, which contains the profound connotation of systematic treatment of complex diseases. AD involves a variety of pathological damage, and the current target drug development model is not ideal, suggesting that more perspectives should be taken in the research and development of AD drugs. Accumulating evidence has demonstrated that TCM could improve cognition, regulate metabolism, inhibit neuroinflammation, reduce oxidative stress and combat aging [31–33]. In contrast to typical singular chemical drugs, TCM is a rather sophisticated system that emphasizes the view of the integrity of the entire human body. Chinese herbal medicine or formulae often incorporate diverse components and interact with multiple targets or channels, which deems them challenging to be studied by traditional research methods [34]. Based on the viewpoint of treating AD from "phlegm", our study proposed that TCM formula NTQ, which was composed of the principle of "dissipating phlegm for resuscitation", focuses on clearing the phlegm in the brain.

Systems pharmacology is a comprehensive approach to understanding disease signaling disturbances and drug modes of action. It has been served as a valuable module to address the complicated and unique mechanism of TCM [35]. In the present study, we employed this method

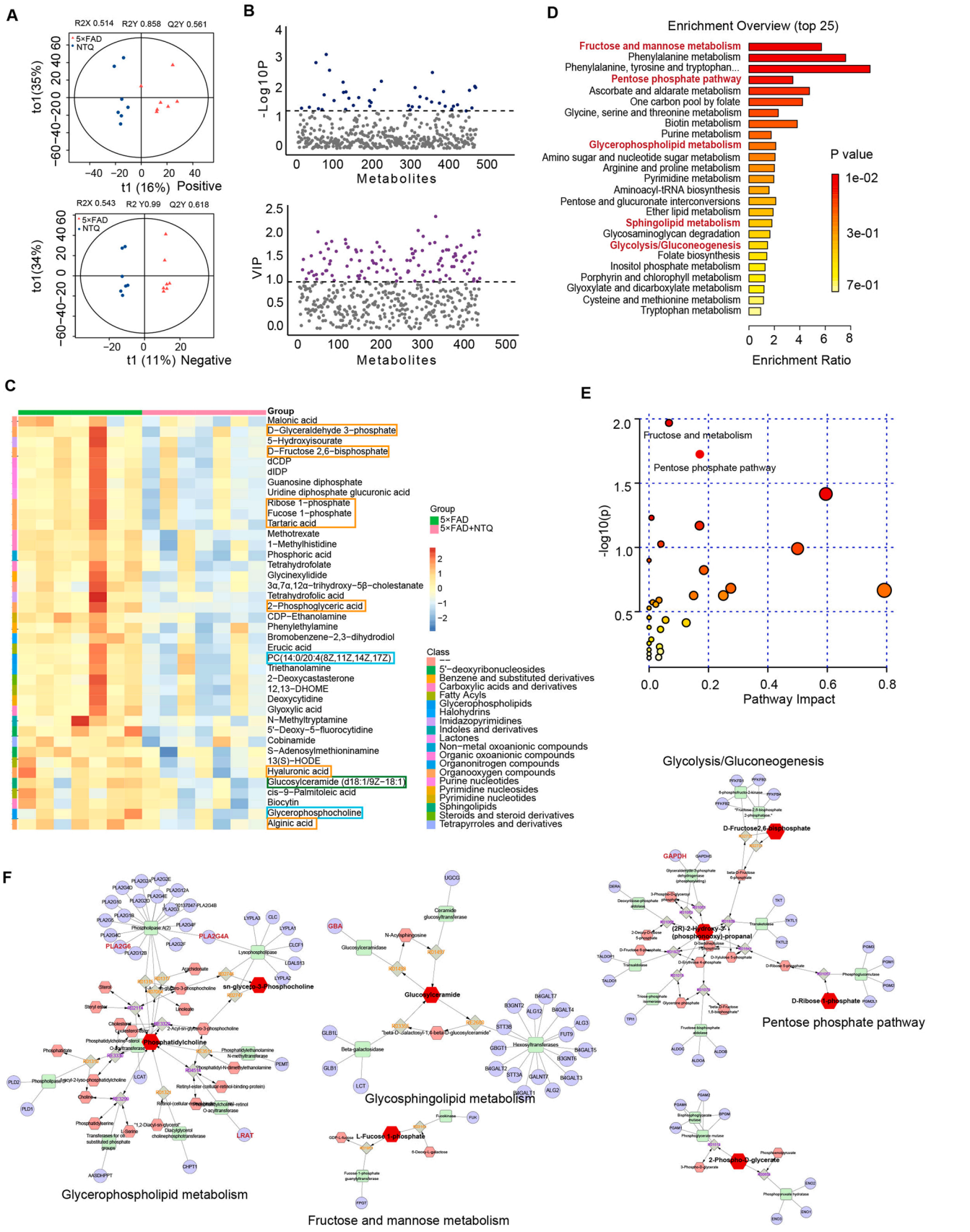

(caption on next page)

Fig. 6. NTQ remodeled metabolic profiling of 5×FAD mice. (A) OPLS-DA (orthogonal partial least-squares discrimination analysis) score plot of NTQ-treated 5×FAD mice *vs.* 5×FAD control mice based on the metabolic profiles. (B) P-value (t-test) and VIP (OPLS-DA) of metabolites in NTQ-treated 5×FAD mice *vs.* 5×FAD control mice. Color was used to encode based on Fold change. (C) The heat maps of significantly changed metabolites in NTQ-treated 5×FAD mice *vs.* 5×FAD control mice. Red denotes higher concentration, while blue denotes lower concentration. (D) KEGG enrichment analysis of significantly changed metabolites between NTQ-treated 5×FAD mice *vs.* 5×FAD control mice. (E) The major NTQ associated metabolism pathways in 5×FAD mice. Pathway analysis was conducted by MetaboAnalyst 5. Pathway impact value determined by the color and size of the circles. Larger bubble represents more important pathway. The darker color of bubbles denotes higher pathway impact value. (F) The networks of key metabolites and targets. Red hexagons represent active components; grey diamonds represent reactions; green round rectangle represents proteins and purple circles represent genes. The key proteins and genes are zoomed in with a pink background.

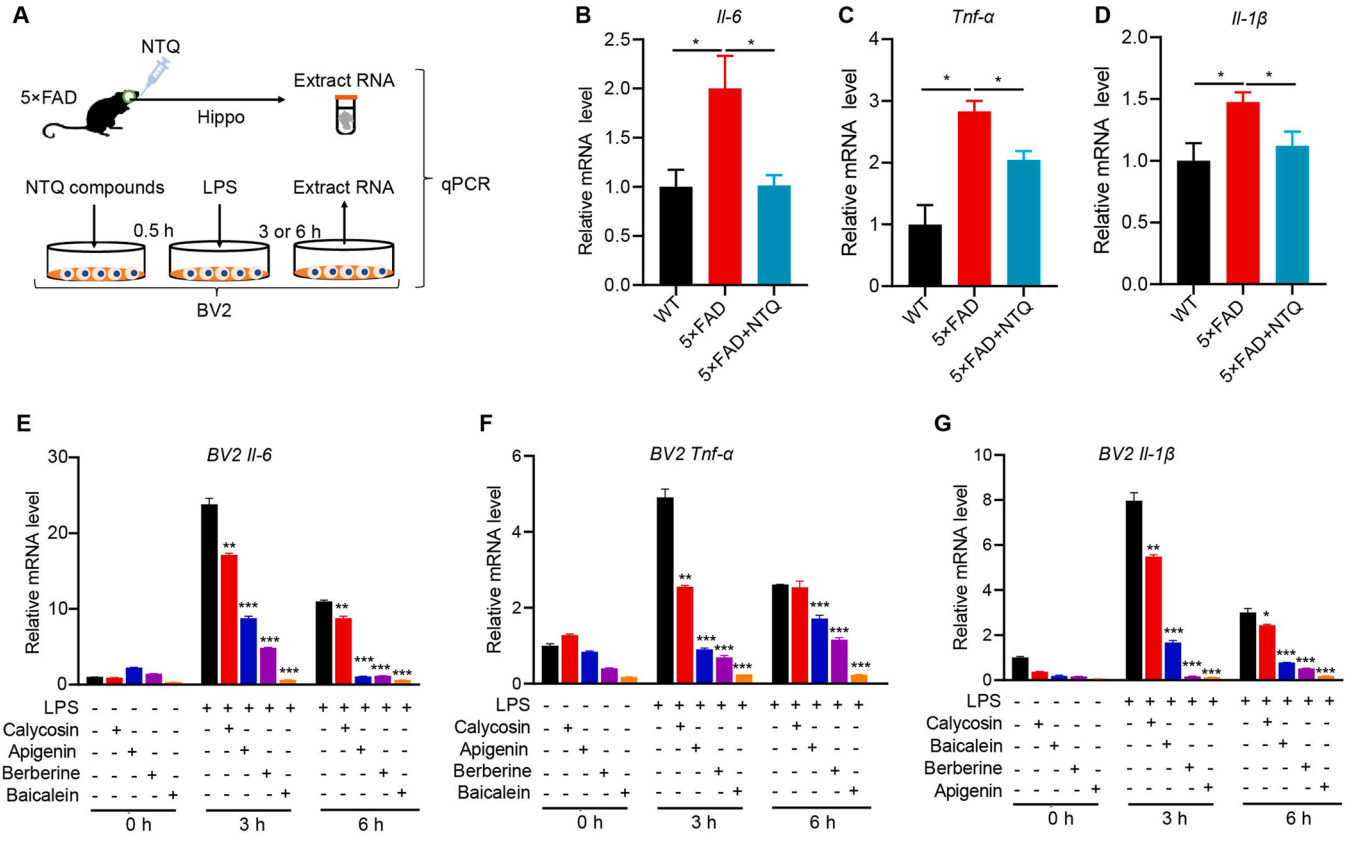

Fig. 7. NTQ reduced the levels of pro-inflammatory factors. (A) Schematic of qPCR analysis for *in vivo* and *in vitro* experiments. (B-D) qPCR analysis showing the *Il-1β*, *Il-6* and *Tnf-α* levels in the hippocampus from indicated group mice (n = 4 per group). (E-G) qPCR analysis showing the *Il-1β*, *Il-6* and *Tnf-α* levels in BV2 cell treated with or without indicated NTQ compounds (n = 3 per group). Data are mean ± SEM. *P < 0.05, * *P < 0.01, * **P < 0.001, * ** *P < 0.0001, one-way ANOVA (B-D), followed by Tukey's multiple comparisons test, or Two-tailed unpaired Student's *t* test (E-G).

(including network pharmacology, transcriptomics, and metabolomics) to investigate the synergistic effects and mechanisms of NTQ. Network pharmacology provided an alternative option to understand the active components and reaction mechanisms of NTQ. Through network pharmacology, we revealed the protective effects of NTQ against AD with the underlying molecular mechanisms. In addition, baicalein, berberine, apigenin and calycosin were identified as the main active ingredients of NTQ. Notably, each of these compounds have been reported to ameliorate cognitive impairment and Aβ pathology in AD animal models [36–41]. Interestingly, we found that the regulation of neuroinflammation and glycolipid metabolism pathways may convey the protective effects of NTQ against AD according to our omics analyses and experimental validation.

Neuroinflammation, an early event of neurodegenerative diseases, is gaining increasing attention in the pathogenesis of AD [42,43]. Glial cells (microglia and astrocytes) have been demonstrated to be responsible for the neuroinflammation *via* NF-κB and Toll-like receptor pathways that involved inflammatory response [44–46], thus inhibition of Aβ-induced glial cells activation thereby reducing neuroinflammation may represent a potentially feasible paradigm for AD treatment. In the present study, our network pharmacology and omics analysis revealed that NTQ could inhibit neuroinflammation through regulating NF-κB and Toll-like receptor pathways. Consistent with the omics and network pharmacology results, our biological experiments validated that NTQ could markedly down-regulated the levels of pro-inflammatory factors and significantly suppressed the activation of glial cells both *in vivo* and *in vitro*.

Several lines of evidence have highlighted that disrupted metabolism is another early event of AD [47,48], and the homeostasis of glycolipid metabolism are crucial for neural integrity, gliosis, and energy consumption. Multiple lines of evidence have shown that there was a strong link between the AD development and systemic disorders of glycolipid metabolism. Previous studies have shown that key intermediates of sphingolipid metabolism are strikingly upregulated in the cortex of AD [49]. Glycerophospholipids are the paramount class of lipid metabolites that have been found to be associated with amyloid and nerve fibers in AD [50]. Our findings showed that sphingolipids and glycerophospholipids metabolism pathways were regulated by NTQ treatment in 5×FAD mice. Furthermore, we provided evidence that there was a closed relationship between glycolipid metabolism and

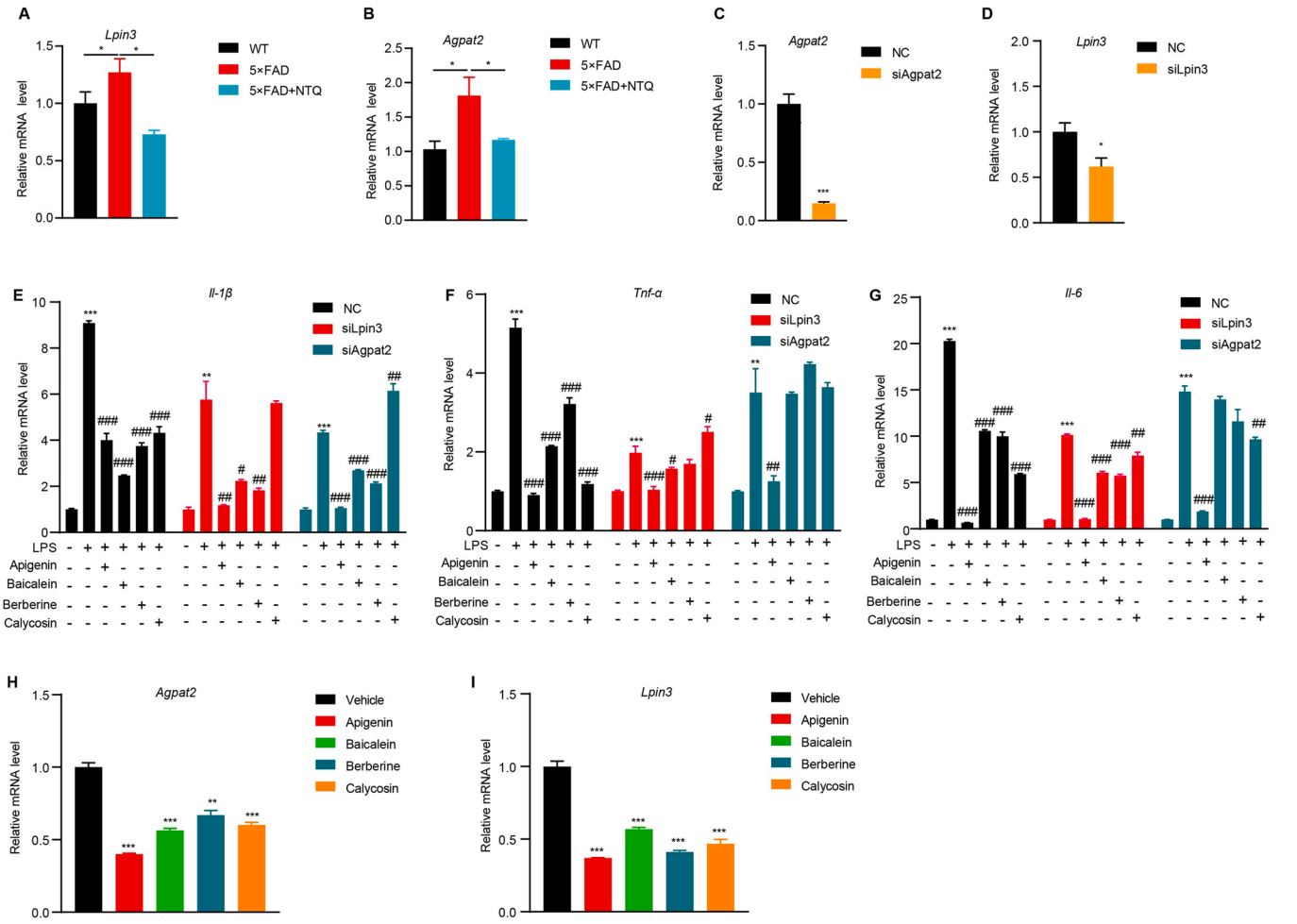

Fig. 8. NTQ inhibited neuroinflammation *via* regulating the expression of *Lpin3* and *Agpat2*. (A, B) Expression levels of *Lpin3* and *Agpat2* in the hippocampus from indicated group mice (n = 4 per group). (C, D) qPCR analysis showing the *Lpin3* and *Agpat2* levels in corresponding siRNA knockdown BV2 cells. (E-G) the *Il-1β*, *Il-6* and *Tnf-α* levels in BV2 cells stimulated by LPS after *Lpin3* and *Agpat2* knockdown. (H, I) qPCR analysis showing the *Agpat2* (H) and *Lpin3* (I) levels in BV2 cells treated with or without indicated NTQ ingredients. Data are mean ± SEM. * , $P < 0.05$; * *, $P < 0.01$; * ** , $P < 0.001$, #, $P < 0.05$; ##, $P < 0.01$; ###, $P < 0.001$. * *vs.* DMSO; # *vs.* LPS. Two-tailed unpaired Student's *t* test (A-D) or one-way ANOVA, followed by Tukey's multiple comparisons test (E-I).

neuroinflammation. Knocking down the key lipid metabolism genes (*i.e.*, *Lpin3* and *Agpat2*) significantly blocked the inflammatory responses of microglial cells. Interestingly, we found that NTQ might inhibit neuroinflammation *via* down-regulating the expression of *Lpin3* and *Agpat2* in AD mice. Therefore, this study highlights an important role of glycolipid pathway in inflammatory responses, and demonstrates that targeting this pathway might represent a potential therapeutic strategy for the treatment of AD as well as other neuroinflammation-associated diseases.

5. Conclusion

In summary, we applied network pharmacology in combination with cellular and animal experiments to demonstrate that NTQ improves AD-like pathology through targeting neuroinflammation and glycolipid metabolism, with implications of NTQ as a potential agent for treating AD.

Funding statement

This work was supported by the National Natural Science Foundation of China (grants No. 81930029 and No. 81630026 to Z.Y., No. U2004201 to F.G. and R-Y.P., No. U21A20414 to Q.H.), the National Major Project of Support Program (grant 2019-JCJQ-ZD-195 to Z.Y.), and the China Postdoctoral Science Foundation (grant No. 2020M683748 to R-Y.P.).

CRediT authorship contribution statement

R.-Y.P., Z.Y. and Q.H. conceived and directed the project. Q.L. and R.-Y.P. designed and performed most of the experiments, analyzed the data, and wrote the manuscript. C.X.J. performed network pharmacology analysis of NTQ. S.L. and Y.L. contributed to data analysis. J.Z., H.W., J.W. and G.L. performed mice genotyping and the Morris water maze. E.L., F.G. and K.Y contributed to revise the manuscript. All authors discussed and commented on the manuscript.

Conflict of interest

The authors declare no conflicts of interest.

Data Availability

Data will be made available on request.

Appendix A. Supporting information

Supplementary data associated with this article can be found in the

online version at doi:10.1016/j.phrs.2022.106489.

References

[1] P. Scheltens, et al., Alzheimer's disease, Lancet 397 (10284) (2021) 1577–1590.
[2] Z.-H. Wang, et al., Deficiency in BDNF/TrkB neurotrophic activity stimulates δ-secretase by upregulating C/EBPβ in Alzheimer's disease, Cell Rep. 28 (3) (2019) 655–669, e5.
[3] P. Giusti-Rodríguez, et al., Synaptic deficits are rescued in the p25/Cdk5 model of neurodegeneration by the reduction of β-secretase (BACE1), J. Neurosci. 31 (44) (2011) 15751–15756.
[4] J.A. Soria Lopez, H.M. González, G.C. Léger, Alzheimer's disease, Handb. Clin. Neurol. 167 (2019) 231–255.
[5] E. Kiss, et al., Artesunate restores the levels of inhibitory synapse proteins and reduces amyloid-β and C-terminal fragments (CTFs) of the amyloid precursor protein in an AD-mouse model, Mol. Cell Neurosci. 113 (2021), 103624.
[6] A. Atri, The Alzheimer's disease clinical spectrum: diagnosis and management, Med Clin. North Am. 103 (2) (2019) 263–293.
[7] Y.J. Dai, et al., Recent advances of traditional Chinese medicine on the prevention and treatment of COVID-19, Chin. J. Nat. Med 18 (12) (2020) 881–889.
[8] F. Lu, et al., Current strategies and technologies for finding drug targets of active components from traditional Chinese medicine, Front Biosci. (Landmark Ed.) 26 (9) (2021) 572–589.
[9] C. Liang, et al., Suppression of MIF-induced neuronal apoptosis may underlie the therapeutic effects of effective components of Fufang Danshen in the treatment of Alzheimer's disease, Acta Pharmacol. Sin. 39 (9) (2018) 1421–1438.
[10] J. Wang, et al., LW-AFC, a new formula derived from liuwei dihuang decoction, ameliorates cognitive deterioration and modulates neuroendocrine-immune system in SAMP8 mouse, Curr. Alzheimer Res. 14 (2) (2017) 221–238.
[11] M. Yi, et al., βIntegrated metabolomic and lipidomic analysis reveals the neuroprotective mechanisms of bushen tiansui formula in an A1-42-induced Rat Model of Alzheimer's disease, Oxid. Med. Cell. Longev. 2020 (2020), 5243453.
[12] H. Pei, et al., Traditional chinese medicine for Alzheimer's disease and other cognitive impairment: a review, Am. J. Chin. Med. 48 (3) (2020) 487–511.
[13] C. Tang, et al., TCM, brain function and drug space, Nat. Prod. Rep. 33 (1) (2016) 6–25.
[14] S. Chen, et al., Traditional Chinese medicine: role in reducing β-amyloid, apoptosis, autophagy, neuroinflammation, oxidative stress, and mitochondrial dysfunction of Alzheimer's disease, Front. Pharmacol. 11 (2020) 497.
[15] Z.H. Lin, Qiu Chang-lin's experience in the differential treatment of senile dementia based on phlegm, J. Tradit. Chin. Med 29 (2) (2009) 131–136.
[16] Y.C. Miao, et al., Effects of Chinese medicine for tonifying the kidney and resolving phlegm and blood stasis in treating patients with amnestic mild cognitive impairment: a randomized, double-blind and parallel-controlled trial, Zhong Xi Yi Jie He Xue Bao 10 (4) (2012) 390–397.
[17] Mehta, K., et al., *Host-directed therapies for tuberculosis: quantitative systems pharmacology approaches.* 2021.
[18] J.T. Jarrell, et al., Network medicine for Alzheimer's disease and traditional Chinese medicine, Molecules 23 (5) (2018) 1143.
[19] A.L. Hopkins, Network pharmacology, Nat. Biotechnol. 25 (10) (2007) 1110–1111.
[20] Mehrpooya, A., et al., *High dimensionality reduction by matrix factorization for systems pharmacology.* 2021.
[21] Asín-Prieto, E., et al., A quantitative systems pharmacology model for acute viral hepatitis B. 2021. 19: p. 4997–5007.
[22] R.Y. Pan, et al., Sodium rutin ameliorates Alzheimer's disease-like pathology by enhancing microglial amyloid-β clearance, Sci. Adv. 5 (2) (2019) eaau6328.
[23] R.Y. Pan, et al., Positive feedback regulation of microglial glucose metabolism by histone H4 lysine 12 lactylation in Alzheimer's disease, Cell Metab. 34 (4) (2022) 634–648, e6.
[24] D. Jeremic, L. Jiménez-Díaz, J. Navarro-López, *Past*, present and future of therapeutic strategies against amyloid-β peptides in Alzheimer's disease a systematic review, Ageing Res. Rev. (2021), 101496.
[25] I.J.Bp I.J.Bp, Neuroinflammation May Indeed Be a Major Player in Opioid Use Disorder in Humans. 2021. 90(8): p. 511–512.
[26] J. Cheng et al. Microglial Calhm2 regulates neuroinflammation and contributes to Alzheimer's disease pathology. 2021. 7(35).
[27] M. Shibuya, et al., Autoantibodies against glial fibrillary acidic protein (GFAP) in cerebrospinal fluids from Pug dogs with necrotizing meningoencephalitis, J. Vet. Med Sci. 69 (3) (2007) 241–245.
[28] Y. Chen, et al., [Effect of fermentation on components of bile acids in Arisaema Cum Bile and determination of three kinds of free bile acids in Arisaema Cum Bile], Zhongguo Zhong Yao Za Zhi 43 (22) (2018) 4457–4461.
[29] Q. Zhao, et al., Simultaneous analysis of twelve bile acids by UPLC-MS and exploration of the processing mechanism of bile arisaema by fermentation, J. Anal. Methods Chem. 2019 (2019), 2980596.
[30] E. Karran J.J.Aon A critique of the drug discovery and phase 3 clinical programs targeting the amyloid hypothesis for Alzheimer disease. 2014. 76(2): p. 185–205.
[31] X. Cheng, et al., LW-AFC, a new formula from the traditional Chinese medicine Liuwei Dihuang decoction, as a promising therapy for Alzheimer's disease: Pharmacological effects and mechanisms, Adv. Pharm. 87 (2020) 159–177.
[32] A. Iyaswamy, et al., NeuroDefend, a novel Chinese medicine, attenuates amyloid-β and tau pathology in experimental Alzheimer's disease models, J. Food Drug Anal. 28 (1) (2020) 132–146.
[33] Y. Guo, et al., Salvia miltiorrhiza improves Alzheimer's disease: a protocol for systematic review and meta-analysis, Med. (Baltim.) 99 (36) (2020), e21924.
[34] S. Wang, et al., Metabolic reprogramming by traditional Chinese medicine and its role in effective cancer therapy 170 (2021), 105728.
[35] M. Chen, Q. Sun, Systemic pharmacology understanding of the key mechanism of Sedum sarmentosum Bunge in treating hepatitis, Naunyn Schmiede Arch. Pharm. 394 (2) (2021) 421–430.
[36] D. Wei, et al., Ameliorative effects of baicalein on an amyloid-β induced Alzheimer's disease rat model: a proteomics study, Curr. Alzheimer Res 11 (9) (2014) 869–881.
[37] X.H. Gu, et al., The flavonoid baicalein rescues synaptic plasticity and memory deficits in a mouse model of Alzheimer's disease, Behav. Brain Res 311 (2016) 309–321.
[38] Z. Cai, C. Wang, W. Yang, Role of berberine in Alzheimer's disease, Neuropsychiatr. Dis. Treat. 12 (2016) 2509–2520.
[39] E. Seo N. Fischer T.J.Pr Efferth Phytochemicals as inhibitors of NF-κB for treatment of Alzheimer's disease. 2018. 129: p. 262–273.
[40] L. Zhao, et al., Neuroprotective, anti-amyloidogenic and neurotrophic effects of apigenin in an Alzheimer's disease mouse model, Molecules 18 (8) (2013) 9949–9965.
[41] L. Song, et al., Calycosin improves cognitive function in a transgenic mouse model of Alzheimer's disease by activating the protein kinase C pathway, Neural Regen. Res. 12 (11) (2017) 1870–1876.
[42] B. Zhang, et al., Integrated systems approach identifies genetic nodes and networks in late-onset Alzheimer's disease, Cell 153 (3) (2013) 707–720.
[43] M.T. Heneka, et al., Neuroinflammation in Alzheimer's disease, Lancet Neurol. 14 (4) (2015) 388–405.
[44] S. Momtazmanesh, G. Perry, N. Rezaei, Toll-like receptors in Alzheimer's disease, J. Neuroimmunol. 348 (2020), 577362.
[45] C. Ju Hwang, et al., NF-κB as a key mediator of brain inflammation in Alzheimer's disease, CNS Neurol. Disord. Drug Targets 18 (1) (2019) 3–10.
[46] B.J. Ding, et al., Soybean isoflavone alleviates β-amyloid 1-42 induced inflammatory response to improve learning and memory ability by down regulation of Toll-like receptor 4 expression and nuclear factor-κB activity in rats, Int. J. Dev. Neurosci. 29 (5) (2011) 537–542.
[47] A. Rijpma, et al., The medical food Souvenaid affects brain phospholipid metabolism in mild Alzheimer's disease: results from a randomized controlled trial, Alzheimer's. Res. Ther. 9 (1) (2017), 51-51.
[48] J.N. Kanfer, et al., Alterations of selected enzymes of phospholipid metabolism in Alzheimer's disease brain tissue as compared to non-Alzheimer's demented controls, Neurochem Res. 18 (3) (1993) 331–334.
[49] M. Yi, et al., Integrated metabolomic and lipidomic analysis reveals the neuroprotective mechanisms of bushen tiansui formula in an Aβ1-42-induced rat model of Alzheimer's disease, Oxid. Med. Cell. Longev. 2020 (2020), 5243453-5243453.
[50] L. Whiley, et al., Evidence of altered phosphatidylcholine metabolism in Alzheimer's disease, Neurobiol. Aging 35 (2) (2014) 271–278.